Supporting Information

Tailoring Fast Directional Mass Transport of Nano-Confined Ag-Cu Alloys upon Heating: Effect of the AlN Barrier Thickness

Vicente Araullo-Peters, Claudia Cancellieri, Mirco Chiodi, Jolanta Janczak-Rusch, Lars P.H. Jeurgens*

Empa, Swiss Federal Laboratories for Materials Science and Technology, Laboratory for Joining Technologies & Corrosion, Ueberlandstrasse 129, 8600 Duebendorf, Switzerland

*Corresponding author: lars.jeurgens@empa.ch, Tel. +41 58 765 4053

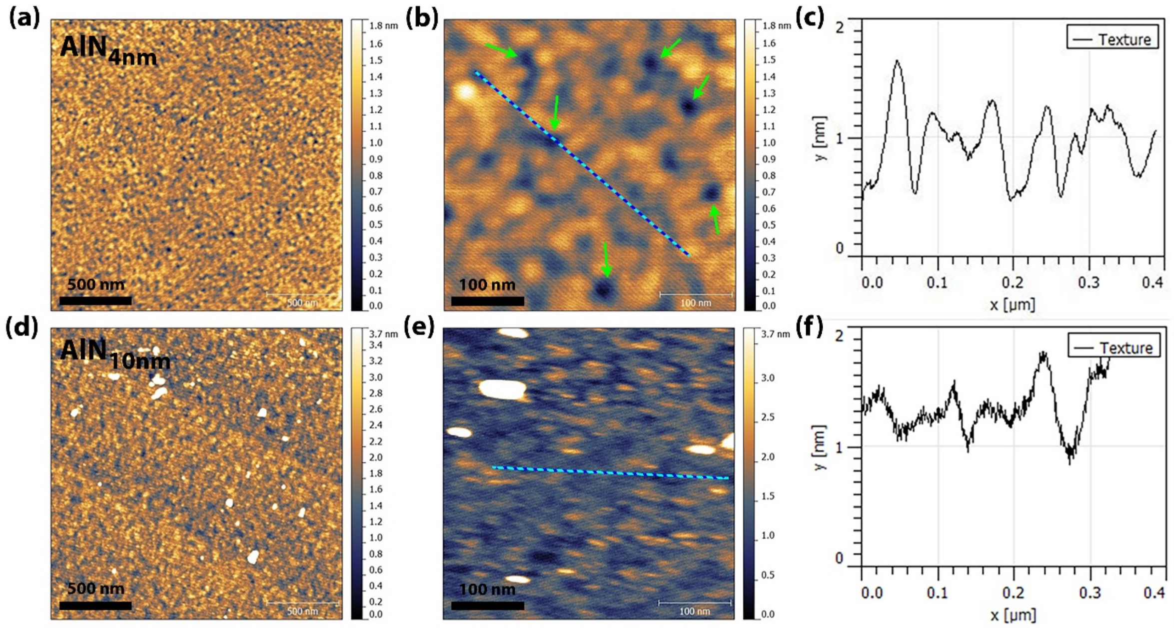

Figure S1. Topographic analysis of the (**a,b,c**) $AgCu_{8nm}|AlN_{4nm}$ NML and the (**d,e,f**) $AgCu_{8nm}|AlN_{10nm}$ NML surface by high-resolution AFM using a Brucker ICON3 with a FMG01/TiN tip (NT-MDT) operating in peak force mode. Pannels (a,d), (b,e) and (c,f) correspond to large-scale area scans, small-scale area scans and line scans, respectively. The dashed lines in (b,e) indicate the positions of the line scans of (c,f). The AFM evidences the presence of tiny nanopores on the AlN_{4nm} surface (as indicated by green arrows in b), which are rather randomly distributed across the NML surface. These nanopores originate from incomplete coalescence of AlN nanograins during the film deposition process, which are characteristic for the initial stages of thin film growth by physical vapour deposition methods (see text for details).

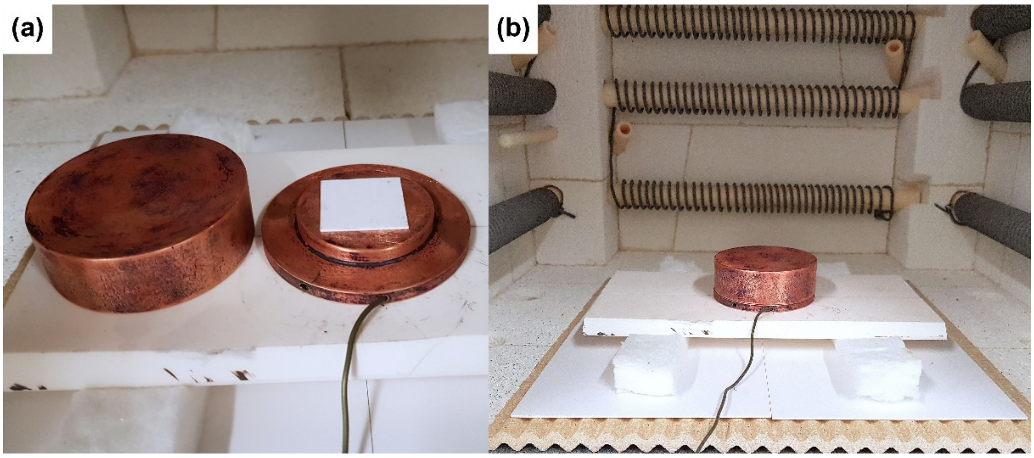

Figure S2. Experimental setup used to achieve (near-)isothermal annealing conditions in air. (a) The specimen was places into a partial open cavity of a massive Cu block, (b) which was positioned and preheated at the desired temperature in a conventional furnace. After the thermal treatment, the specimen was removed from the Cu block and allowed to cool in air.

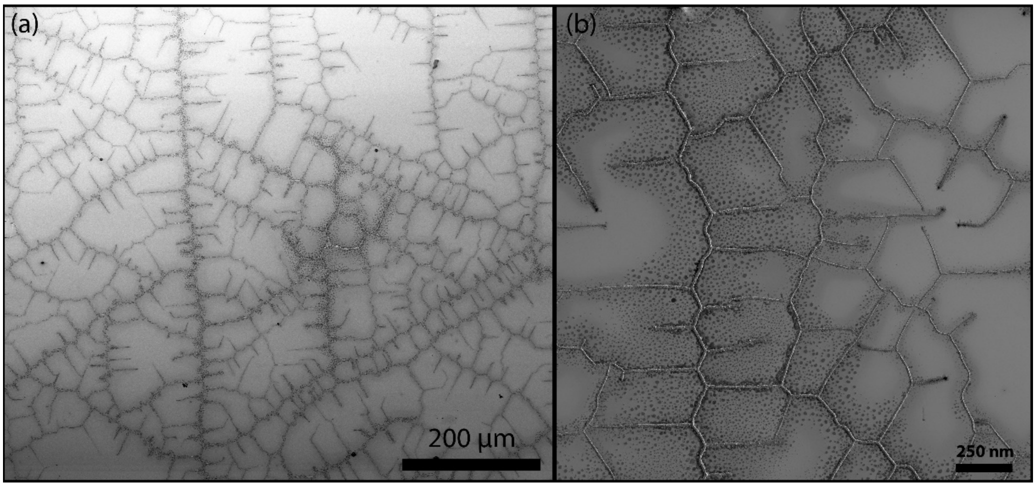

Figure S3. (**a,b**) Secondary electron images of the surface of the $AgCu_{8nm}|AlN_{10nm}$ NMLs after 5 min of isothermal annealing at 400 °C, showing a widespread network of line-shapes protrusions on the annealed NML surface. These line-shaped networks form a hexagonal network with angles of 120° between the contacting lines and are adjoined by numerous dark patches, which correspond to confined voids in the NML. The size and density of these confined voids roughly decreases with decreasing distance perpendicular to the lines. Moreover, the higher the density of lines, the higher the density of dark patches.

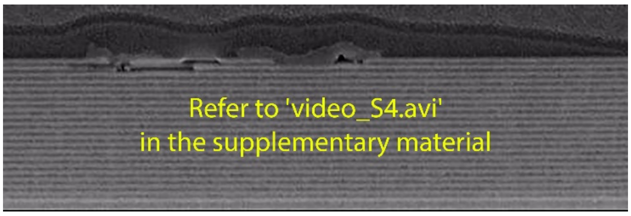

Video S4. Video showing a series of cross-sectional SEM images obtained by cross-sectional FIB slicing along the direction of a typical line-shape feature. The data pertains to an $AgCu_{8nm}|AlN_{10nm}$ NMLs after 5 min of isothermal annealing at 400 °C. The cross-sectional FIB slicing with imaging clearly evidences that the Cu, which forms the line-shaped protrusions, preferentially originates from the topmost alloy NLs. Nevertheless, at several locations, the cracks extend throughout the entire NML thickness and are covered by relative large Cu- protrusions, as illustrated in Video S5.

Video S5. Video showing a series of cross-sectional SEM images obtained by cross-sectional FIB slicing through an extended crack and its associated relatively large Cu(O) protrusion on top. The data pertains to an $AgCu_{8nm}|AlN_{10nm}$ NMLs after 5 min of isothermal annealing at 400 °C. The cross-sectional FIB slicing with imaging clearly evidences that the Cu, which forms the large protrusions, originates from the entire NML adjacent to the crack.